3.0 Air-sea CO_2 fluxes

3.1 Data collection

Between March 1995 and March 1999, CO_2 measurements were continuously made using underway CO_2 partial pressure (pCO_2) systems during 68 crossings in the northern North Pacific Ocean aboard M/S *Skaugran* (Zeng *et al.*, 2002). Most transects from North America to Japan followed a great circle route through the Gulf of Alaska and Bering Sea, then southward along the Kuril Islands. Routes between Japan and North America ranged from 34°N and 50°N in the central North Pacific, except one passing though Hawaii (Fig. 2). Measurements for seawater were taken every minute, and hourly for air, in the units of the mole fraction of CO_2.

For every crossing, the means of the 1-min CO_2 data were averaged for each 1° of longitude. 5° means were computed from the 1° means for data between 145°E and 125°W. In order to avoid the strong effects of regional variability in near-shore waters, the 5° means at the route extremes (145°E and 125°W) were calculated using data between 145°E and 147.5°E, and between 125°W and 127.5°W due to their one-sidedness.

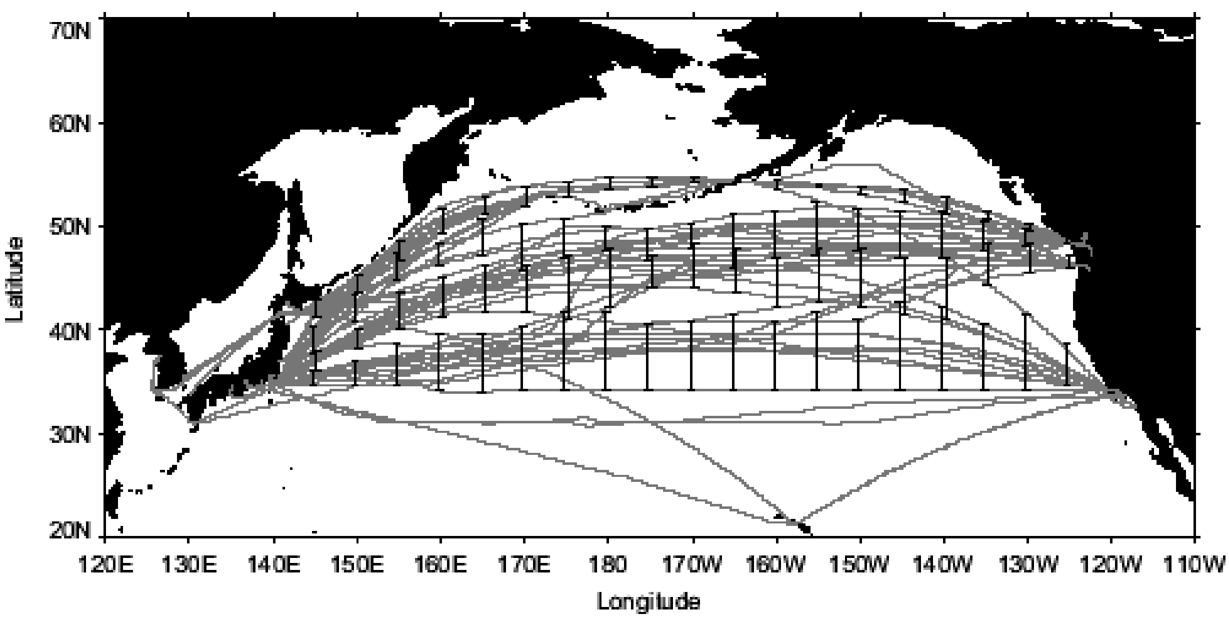

Fig. 2 Ship routes of M/S *Skaugran* from March 1995 to March 1999. Vertical lines intersecting ship routes mark the selected latitudinal bands for estimating coefficients of the seasonal function of pCO_2 using Eq. (2).

3.2 Data analysis

Nojiri *et al*. (1999) evaluated seasonal ΔpCO_2 at 5° x 5° resolution using a function consisting of four harmonic terms. This function contains a linear latitudinal gradient term independent of time, and utilized data that were collected between 1995 – 1997. By using a longer 4-year time series, Zeng *et al.* (2002) found that the north–south gradient varied significantly with time and longitude. Therefore, they omitted the latitudinal gradient term in the model of Nojiri *et al*. (1999), and instead only used the harmonic function:

$$\Delta pCO_2\,(t) = c_o + c_1 \sin(2\pi t) + c_2 \cos(2\pi t) + c_3 \sin(4\pi t) + c_4 \cos(4\pi t) \quad (2)$$

to describe the seasonal ΔpCO_2 changes with time in a box of limited latitude and longitude. This is a spatially independent function requiring that the seasonal coverage of sampling be complete in the defined boxes, and therefore, the box size was chosen as a compromise between maximizing seasonal coverage and minimizing the spatial variations within each box.

In order to assure that there is at least one crossing per season, the box sizes were selected as follows: for each 5° longitudinal section, latitudinal bands were chosen within which intervals between any two crossings were less than three months. Two bands encompassing the northern and southern boundaries were selected first, after which two additional bands were inserted between the boundaries. The constraint for the maximum latitudinal range is 10°. Figure 2 shows the selected boxes with variable latitude range and fixed longitude range. When examining the monthly route maps, the latitudinal sampling distribution shown in Figure 2 is uneven, *i.e.*, there is only one crossing in the area of 170°E – 160°W and 35°N – 40°N during July – September.

The seasonal cycle of ΔpCO_2 (i.e., the coefficients c_o through c_4) were defined for each box using Eq. (2). Figure 3 shows the results for the 175°W section as an example of this selection and calculation process. Four latitudinal bands were selected for this longitude section, and the seasonal cycle of ΔpCO_2 is displayed for each box. The interpolation to 1° x 1° monthly resolution from the irregular grid of distributions of ΔpCO_2 (as shown in Fig. 2) allows computation of basin-wide fluxes and facilitates comparison with other regional estimates of ΔpCO_2 and fluxes.

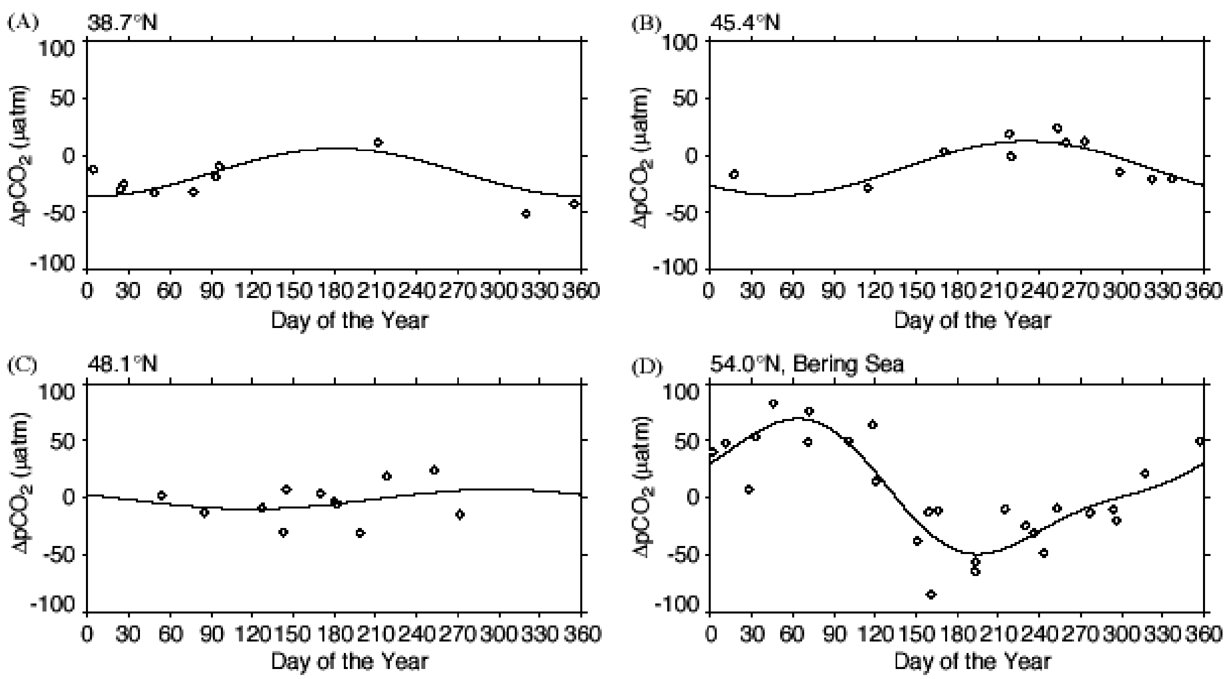

Fig. 3 Seasonal functions of ΔpCO_2 for four latitudinal bands in the 175°W longitudinal section: (A) 38.7°N; (B) 45.4°N; (C) 48.1°N; and (D) 54.0°N. The solid line shows the seasonal function fit by Eq. (2); the diamond symbol shows the observed data.

3.3 CO_2 fluxes

Based on Eq. (2) of Wanninkhof (1992), the air-sea flux of CO_2 was calculated from wind speed. Monthly CO_2 fluxes were computed using monthly ΔpCO_2, monthly sea-surface temperature and salinity of World Ocean Atlas 1994 of National Oceanic and Atmospheric Administration (NOAA), and the monthly wind fields derived from the European Center for Medium-Range Weather Forecasts (ECMWF) 2.5° database. The ECMWF database contains winds (at 10 m height above sea surface) for every 12 hours. The monthly wind fields are means of 12-hour winds in January 1995 – December 1999.

Clear unsynchronized patterns of ΔpCO_2 changes were observed for different regions in the northern North Pacific. For the northern regions, ΔpCO_2 is highest in winter and lowest in summer. For the subtropics, this seasonal cycle is reversed, with lowest values in winter and highest values in summer. Due to vertical mixing in winter (January – March), seawater pCO_2 in the southern Bering Sea, off Kamchatka Island, and off the Kuril Islands is higher than in the atmosphere (by up to +80 μatm). In the remainder of the northern North Pacific, ΔpCO_2 is negative (by as much as –60 μatm), more than likely a result of seasonal cooling.

CO_2 fluxes from this analysis were compared with fluxes computed from the data of Takahashi *et al*. (1997). In order to compare results with 4° x 5° grid, their 1° x 1° data were averaged to this larger grid, and thus, fluxes for both studies were calculated using the same resolution of ΔpCO_2. Using that approach, both data sets show that the northern North Pacific is a net CO_2 sink throughout the year, weakest in summer (July – September) and strongest in autumn (October – December). The monthly mean CO_2 flux ranges between –0.06 and –4.7 moles m^{-2} yr^{-1}, with the negative sign indicating ocean uptake. Comparison of monthly mean fluxes for the northern North Pacific indicates that in spring (April – June) and autumn (October – December), monthly fluxes estimated from ΔpCO_2 of Takahashi *et al*. (1997) are systematically more negative than those estimated by Zeng *et al.* (2002); *i.e*., on average 17% lower (–15 to –20%) in spring and 44% lower (–25% to –56%) in autumn.

Based on the ΔpCO_2 results, the region between 34°N and 50°N is estimated to be a small sink for carbon of –0.26 Pg C yr^{-1} (Zeng *et al*. 2002), while the integrated net annual flux using the data of Takahashi *et al*. is –0.33 Pg C yr^{-1}, suggesting 27% more uptake on an annual basis.

The vessel-of-opportunity measurement program aboard commercial vessels offers sampling frequency throughout all seasons, enabling the oceanographic community to better understand the long-term variability of the ocean carbon cycle.